Endorectal magnetic resonance imaging of prostatic cancer: comparison between fat-suppressed T2-weighted fast spin echo and three-dimensional dual-echo, steady-state sequences

Ikonen, S.

2001

Ikonen , S , Kärkkäinen , P , Kivisaari , L , Salo , J O , Taari , K , Vehmas , T , Tervahartiala , P & Rannikko , S 2001 , ' Endorectal magnetic resonance imaging of prostatic cancer: comparison between fat-suppressed T2-weighted fast spin echo and three-dimensional dual-echo, steady-state sequences ' , European Radiology , vol. 11 , no. 2 , pp. 236-241 . https://doi.org/10.1007/s00

http://hdl.handle.net/10138/297734
https://doi.org/10.1007/s003300000598

publishedVersion

Eur. Radiol. (2001) 11: 236–241

S. Ikonen
P. Kärkkäinen
L. Kivisaari
J. O. Salo
K. Taari
T. Vehmas
P. Tervahartiala
S. Rannikko

Endorectal magnetic resonance imaging of prostatic cancer: comparison between fat-suppressed T2-weighted fast spin echo and three-dimensional dual-echo, steady-state sequences

Received: 2 December 1999
Revised: 3 July 2000
Accepted: 4 July 2000

S. Ikonen ✉ · L. Kivisaari · P. Tervahartiala
Department of Radiology,
Helsinki University Central Hospital,
P. O. Box 340, 00029 HUS, Helsinki,
Finland

J. O. Salo · K. Taari · S. Rannikko
Department of Urology, Helsinki
University Central Hospital,
P. O. Box 580, 00029 HUS,
Helsinki, Finland

P. Kärkkäinen
Department of Pathology,
Helsinki University Central Hospital,
P. O. Box 401, 00029 HUS, Helsinki,
Finland

T. Vehmas
Finnish Institution of Occupational Health,
Topeliuksenkatu 41 aA, 00250 Helsinki,
Finland

Abstract The aim of this study was to develop an endorectal MRI strategy for prostatic cancer. We evaluated the MR images from 44 consecutive prostatic cancer patients treated by radical prostatectomy. Each sequence from every examination was assessed separately with a specific tumor map drawn. Tumor localization, capsular penetration, and seminal vesicle invasion were marked on maps on the basis of T2 and DESS (dual-echo steady-state) sequences. Thirty patients also had T1-weighted images, and these were assessed with regard to possible tumor outgrowth. The maps were compared with histopathological findings from radical prostatectomy specimens. According to our study, DESS equaled T2 in every respect. No statistically significant differences between the sequences were found with respect to detecting either tumor localization, outgrowth, or seminal vesicle invasion. DESS is a potential new sequence in prostatic MRI as it has been proven to parallel the routinely used T2-weighted imaging.

Key words Prostate · Prostate neoplasms · MR · Comparative studies

Introduction

Prostate cancer has become a major health care issue for elderly men. Appropriate choice of treatment depends on stage of disease. Thus far, endorectal MRI has appeared to be the most promising imaging method in staging this disease [1, 2, 3, 4], and consequently MRI has become a frequent part of clinical evaluation.

In 1995 we began endorectal MR imaging of prostatic cancer with a T2-weighted fat-suppressed fast spin-echo (FSE) sequence in three dimensions. A T1-weighted sequence was included later to rule out post-biopsy changes which might interfere with image interpretation [5]. In the pelvic region, FSE MR imaging has been shown to be superior to conventional imaging [6, 7]. The time saved can be utilized to attain a higher-resolution matrix with an increased number of signal averages [6] and to allow longer repetition and echo times to increase signal intensity and contrast [7]. The substantial reduction in imaging time also allows use of fat suppression, which results in expansion of the dynamic range for relative signal intensity display on MR images, thus improving tissue contrast. Fat suppression also results in reduction of motion artifacts and elimination of

Table 1 Parameters of sequences used in this study

	T2	DESS	T1
TR (ms)	6000.0	26.8	600.0
TE (ms)	112.0	9.0	17.0
Slice thickness (mm)	3	1.5/2.8[a]	3
Gap (mm)	1.2	0	0.75
FOV (mm)	150 × 150	158 × 180	125 × 125
Matrix	240 × 256	202 × 256	256 × 256
Acquisitions	2	1	2
Duration (min)	3.18	5.26	5.10

[a]In 29 of the patients slice thickness used was 1.5 mm, and in 15 it was 2.8 mm

chemical shift misregistration artifacts. On the other hand, inhomogeneous suppression may degrade image quality. Another disadvantage is the loss of approximately 15 % of the slices compared with regular SE imaging [8, 9]; thus, coverage of a large prostate and seminal vesicles with one set of slices may become impossible.

A DESS sequence makes one averaged image from two separate gradient-echo sequences, of which one produces images with mixed T1- and T2-weighting and the other with heavy T2-weighting [10]. It thus produces high anatomical detail and a high signal from fluid within the same image with excellent spatial resolution, and a high contrast and signal-to-noise ratio. The main problem with DESS is that it is susceptible to motion artifacts. Because the imaging of the prostate gland is performed with a small field of view, only motility of the bowel usually turns out to be disturbing.

With new diagnostic methods, examination costs per patient tend to increase. In order to find a more effective imaging scheme, we evaluated three sequences we routinely use in prostatic MR imaging. Fat-suppressed T2-weighted FSE and 3D DESS imaging were compared to detect tumor localization and seminal vesicle invasion. In addition, both these and a T1-weighted sequence were assessed to discover capsular penetration of the tumor.

Materials and methods

Patient characteristics

We retrospectively reviewed MR images of 44 consecutive prostate cancer patients (mean age 62 years, age range 55–74 years) treated with a radical retropubic prostatectomy from February 1996 to October 1997. Clinical evaluation included patient history, physical examination, serum prostate specific antigen (PSA) determination, transrectal US-guided sextant biopsies, bone scan, and endorectal MRI. Mean serum PSA was 12 g/l (range 0.1–51 g/l). The interval between biopsy and MRI was greater than 3 weeks in all but one case, and the mean interval between MRI and prostatectomy was 31 days (range 1–70).

MR imaging

Magnetic resonance imaging was performed with a 1.5-T superconducting magnet (Vision, Siemens, Erlangen, Germany) with a disposable endorectal prostate coil (MRInnervu Disposable Endorectal Prostate Coil, Medrad, Pittsburgh, Pa.). We obtained T2-weighted fat-suppressed FSE images in the axial, coronal, and sagittal planes, and 3D DESS images were obtained in the axial direction. Of the T2 sequences only axial images were included in the retrospective interpretation. Of the 44 patients, 30 were also imaged with an axial T1-weighted sequence. The parameters of the sequences appear in Table 1. Phase encoding from right to left was used to reduce artifacts caused by motility of the bowel.

Image interpretation

A retrospective analysis of the MR images was performed by two radiologists (S. I. and L. K.) independently in random order. Each sequence was interpreted separately. Radiologists were unaware of the clinical data except that all patients had a biopsy-proven, clinically localized prostate cancer. Tumor localization, capsular penetration, and seminal vesicle invasion were marked on standard tumor maps on the basis of both T2 and DESS images. On the maps, the prostate was divided into the base, body, and apex. The body of the prostate was further divided into eight segments equal in size for more precise tumor localization. The capsule was divided into the base, right, and left halves, and the apex. The seminal vesicles were considered to be one segment. The division of the prostate is described in more detail in our previous study [11]. T1-weighted images were assessed only with regard to possible extracapsular extension of the tumor.

Our criterion for cancer in the peripheral zone was a low signal intensity focus. In the central region, which consisted of the central and transitional zones, a ground-glass-like, homogenous low signal intensity area was considered as tumor. A localized bulge with an irregular margin or direct tumor extension into periprostatic soft tissue was defined as capsular penetration. The neurovascular bundles were also examined as a possible site of extracapsular extension of the tumor. The criterion for seminal vesicle invasion was low signal intensity focus in normally bright vesicular tissue. These criteria were derived from our own experience and the literature [12, 13, 14].

Pathological evaluation

Radical retropubic prostatectomy was performed in all patients, with modified pelvic lymphadenectomy added to exclude pelvic lymph node metastasis. After surgical removal, the intact prostate and seminal vesicles were coated over their entire external surface with silver and fixed in formalin for 2–4 days. After fixation, the right prostatic lobe was marked with an incision. The seminal vesicles as well as apical and basal urethral margins were removed for histological evaluation. The remaining whole prostate was step sectioned at 5-mm intervals. All sections were designated to permit the localization of each section within the prostate. After paraffin embedding, all slides were stained according to the Herovici-van Gieson method. Sections were examined by a single pathologist (P. K.), and cancer areas outlined with a pen. These microscopic findings were then marked on standard tumor maps. Tumor maps drawn by the radiologists and the pathologist were compared segment by segment with regard to cancer localization, capsular penetration, and seminal vesicle invasion.

Table 2 Detection of tumor localization with T2 and DESS sequences

	Accuracy (%)	Sensitivity (%)	Specificity (%)
T2			
Radiologist 1	251 of 440 (57)	123 of 262 (47)	128 of 178 (72)
Radiologist 2	242 of 440 (55)	137 of 262 (52)	105 of 178 (59)
Total	493 of 880 (56)	260 of 524 (50)	233 of 356 (65)
DESS			
Radiologist 1	263 of 440 (60)	129 of 262 (49)	134 of 178 (75)
Radiologist 2	253 of 440 (58)	145 of 262 (55)	108 of 178 (61)
Total	516 of 880 (59)	274 of 524 (52)	242 of 356 (68)

No significant difference between sequences was found at a significance level of $p < 0.05$

Table 3 Detection of seminal vesicle invasion with T2 and DESS sequences

	Accuracy (%)	Sensitivity (%)	Specificity (%)
T2	77 of 88 (88)	3 of 6 (50)	74 of 82 (90)
DESS	80 of 88 (91)	6 of 6 (100)	74 of 82 (90)

No statistical difference between groups existed because of the small number of positive cases

Table 4 Detection of capsular penetration with T1, T2, and DESS sequences

	Accuracy (%)	Sensitivity (%)	Specificity (%)
T1	222 of 240 (93)	2 of 12 (17)	220 of 228 (96)
T2	335 of 352 (95)	4 of 18 (22)	331 of 334 (99)
DESS	333 of 352 (95)	5 of 18 (28)	328 of 334 (98)

No significant difference between groups was found at a significance level of $p < 0.05$

Statistical analysis

Contingency (2×2) tables showed the association between MRI and histopathological findings. In order to determine the difference in sensitivity and specificity in localizing cancer foci between T2 and DESS sequences, we performed McNemar's test for matched samples [15]. To test the differences in sensitivity and specificity in detecting capsular penetration between all the three sequences we performed an extended chi-square test because the numbers of observations per sequence did not remain constant. To evaluate interobserver agreement we used kappa statistics, and we interpreted kappa values according to Altman [16].

Results

Accuracy in locating the tumor in agreement with the pathologist was 56% with the T2 sequence and 59% with DESS. Sensitivity and specificity for T2 were 50 and 65%, and for DESS 52 and 68%, respectively (Table 2).

Histopathological examination showed tumor invasion into the seminal vesicles in 3 patients (7%). Accuracy for detecting vesicle invasion was 88% for T2 and 91% for DESS. The sum of positive, negative, false-positive, and false-negative cases from the readings performed by two radiologists were 3 positive, 74 negative, 8 false-positive, and 3 false-negative cases with T2, and 6, 74, 8, and 0 with DESS (Table 3).

Pathological analysis revealed capsular penetration in 7 of the 44 patients (16%, 9 of 176 possible sites). Accuracy in discovering tumor outgrowth was 95% for both T2 and DESS, and 93% for T1. The sum of positive, negative, false-positive, and false-negative cases from the readings performed by two radiologists were 4 positive, 331 negative, 3 false-positive, and 14 false-negative cases with the T2 sequence; 5, 328, 6, and 13 with DESS; and 2, 220, 8, and 10 with the T1 sequence (Table 4).

Interobserver consistencies were calculated for detecting cancer localization, capsular penetration, and seminal vesicle invasion, and agreement rates ranged from fair to very good (Table 5).

Discussion

Why did we start using DESS instead of the fat-suppressed T2 FSE sequence? Firstly, we began to suspect that fat-suppression may lead to reduced definition of periprostatic anatomic tissue planes as Mirowitz et al. have also stated [9]. As a consequence, our ability to detect tumor outgrowth might be limited. With DESS, the signal intensity of periprostatic fat is higher, and we assumed that with this technique relatively low signal intensity extracapsular prostate cancer might be better visualized. Secondly, with DESS we can definitely cover the whole prostate gland and also the seminal vesicles with one set of slices. As a 3D sequence, DESS images the whole prostate without any gap. Because the slices obtained are thinner, misinterpretations caused by partial-volume effect can be diminished. Moreover, 3D im-

Table 5 Kappa values of interobserver agreement rates

	Tumor localization		Seminal vesicle invasion		Capsular penetration		
	T2	DESS	T2	DESS	T2	DESS	T1
Radiologist 1 vs radiologist 2	0.36	0.44	0.68	0.64	0.92	0.92	0.90

Kappa values were interpreted as poor –0.20 or less, fair –0.21 to 0.40, moderate –0.41 to 0.60, good –0.61 to 0.80, and very good –0.81 to 1.00

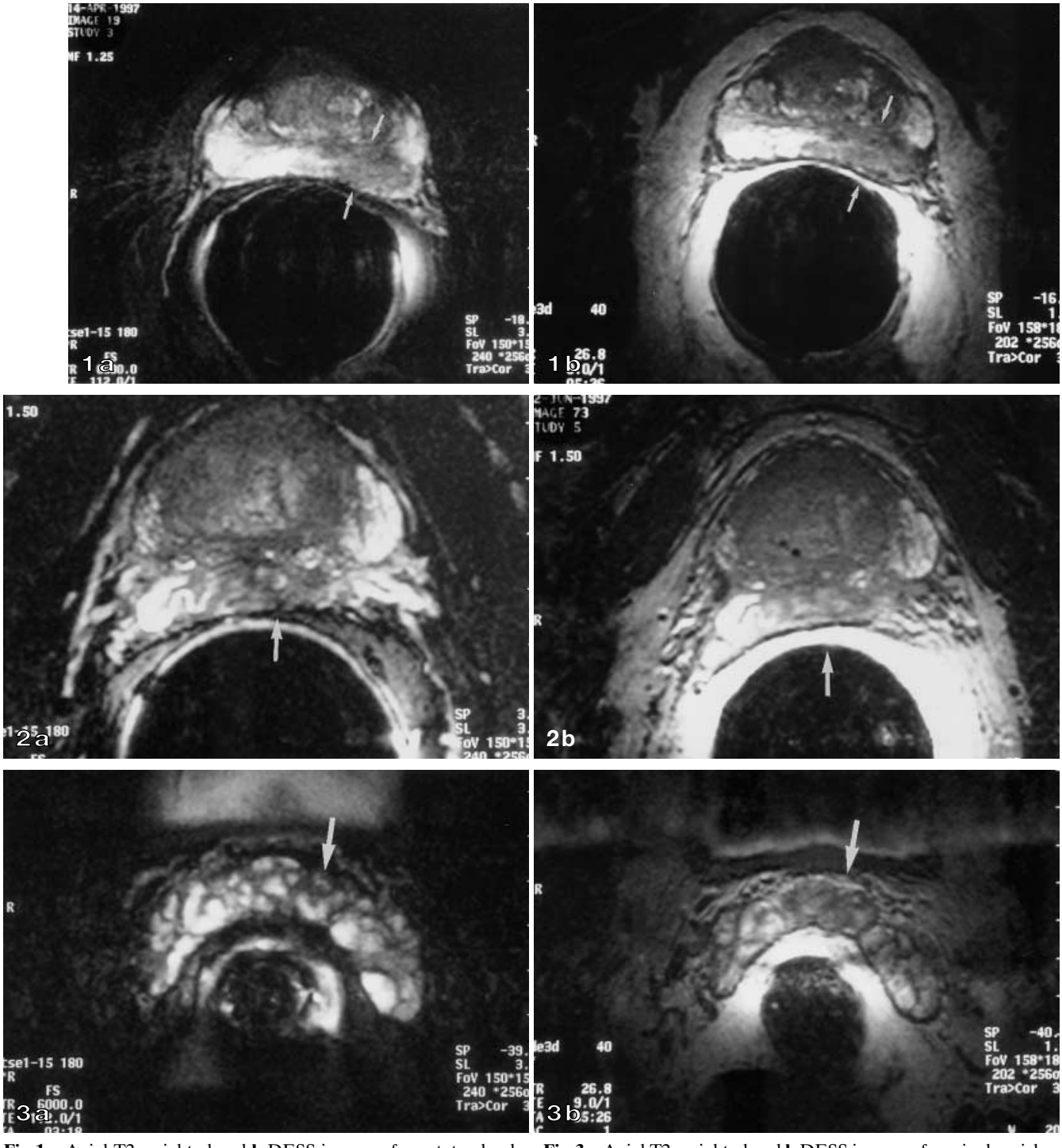

Fig. 1 a Axial T2-weighted and **b** DESS images of prostate gland. Both images show the site of carcinoma as decreased signal intensity in the left peripheral zone *(arrows)*

Fig. 2 a Axial T2-weighted and **b** DESS images. Both demonstrate extensive carcinoma which fills nearly the whole prostate and invades also the seminal vesicles *(arrows)*

Fig. 3 a Axial T2-weighted and **b** DESS images of seminal vesicles. T2 shows thickened wall of the vesicles. Clear invasion of the tumor is seen in DESS *(arrows)*

aging makes it possible to perform reconstructions in different directions with no need to image the prostate in multiple planes. Our third assumption was that, as both DESS and T2-weighted imaging are sensitive to those tissues with a long T2 relaxation time, low signal intensity cancer lesions could be easily detected in the normal high signal intensity peripheral zone.

Small tumors were not excluded from this study, although we reported previously [11] that detection of cancer foci < 5 mm in diameter is difficult. The reason was that we expected DESS to prove more sensitive than T2 in localizing tumors; however, no significant difference appeared. Probably such small tumors are just beyond our detection with the current technology.

According to our study, both T2 and DESS demonstrate the tumor foci equally (Figs. 1, 2). With T2, our accuracy in localizing tumor foci was 56 % and with DESS 59 %. Jager et al. [17] reported a 67 % accuracy in localizing tumors, and in our own previous study [11] accuracy was 61 %. Jager et al. obtained an axial T1-weighted sequence, and axial, sagittal, and coronal T2-weighted images. In our previous study T1-weighted images were not included, but T2-weighted images were acquired in all three directions. In the present study 30 of the patients were imaged also with a T1-weighted sequence, but during the retrospective analysis, sequences were interpreted separately. We had a large number of false-positive findings in localizing tumor foci, partly because of the misinterpreted postbiopsy changes. The number of false-positive findings could have been reduced had the sequences been examined together.

DESS seems to be more sensitive than T2-weighted imaging in discovering seminal vesicle invasion (50 vs 100 %; Fig. 3); however, we failed to demonstrate any statistically significant difference between the two sequences. This may reflect uncertainty associated with the small number of positive cases in our material. The problem with studies in which prostatectomy specimens act as the gold standard is the so-called verification bias. To obtain histopathological evidence, the patient has to be surgically treated. As patients with clear extraprostatic tumor growth do not undergo radical prostatectomy, the population becomes selected. The demonstration of a possibly statistically significant difference between our imaging sequences in detecting seminal vesicle invasion would thus require a considerably larger series. In recent studies by Perrotti et al. [18] and Jager et al. [17], sensitivities for vesicle invasion were 23 and 36 %, respectively. Specificities were 93 and 89 %. Our specificity was 90 % for both T2 and DESS.

In their study, Perrotti et al. [18] reported sensitivity of 22 % and specificity of 84 % for invasion of periprostatic soft tissue, whereas Jager et al. [17] achieved 43 and 84 %, respectively. Our corresponding figures were 22 and 99 % for T2, 28 and 98 % for DESS, and 17 and 96 % for T1. Yu et al. [19] stated that obliteration of the rectoprostatic angle and asymmetry of the neurovascular bundles were the most indicative features of extracapsular extension. T1-weighted images in the present study were analyzed to determine whether they made the neurovascular bundles more conspicuous and thus would be of any help in the detection of capsular penetration. The interpretation of T1-weighted images was somewhat arbitrary; because the images were examined separately, intraprostatic tumors of these patients could not be localized to help the detection of capsular penetration.

We did not use 3D capabilities of DESS while analyzing the material, but an additional benefit may be obtained by using them. We performed multiplanar reconstructions with DESS, and resolution seemed sufficient with 1.5-mm slice thickness. Image survey proved to be quick in all three planes at the computer work station.

Kappa values of interobserver agreement rates were consistent between T2 and DESS. Overall, agreement rate was weakest in detecting tumor localization and best in detecting capsular penetration, the latter being very good.

Conclusion

Based on our results, DESS seems to be equal to T2-weighted imaging and may be even more sensitive with regard to detecting seminal vesicle invasion. As a result, we plan to give up the routinely used T2-weighted sequence in our imaging scheme of the prostate gland to reduce the total imaging time. We still consider T1-weighted images necessary to rule out artifacts caused by postbiopsy hemorrhage.

Acknowledgements We thank the Institute of Helsinki University Central Hospital for financial support.

References

1. Rifkin MD, Zerhouni EA, Gatsonis CA, Quint LE, Paushter DM, Epstein JI, Hamper U, Walsh PC, McNeil BJ (1990) Comparison of magnetic resonance imaging and ultrasonography in staging early prostate cancer. N Engl J Med 323:623–626
2. Platt JF, Bree RL, Schwab RE (1987) The accuracy of CT in the staging of carcinoma of the prostate. AJR 149:315–318
3. Bates TS, Gillat DA, Cavanagh PM, Speakman M (1997) A comparison of endorectal magnetic resonance imaging and transrectal ultrasonography in the local staging of prostate cancer with histopathological correlation. Br J Urol 79:927–932

4. Böni RAH, Boner JA, Debatin JF, Trinkler F, Knönagel H, Hochstetter A von, Helfenstein U, Krestin GP (1995) Optimization of prostate carcinoma staging: comparison of imaging and clinical methods. Clin Radiol 50:593–600
5. White S, Hricak H, Forstner R, Kurhanewicz J, Vigneron DB, Zaloudek CJ, Weiss JM, Narayan P, Carroll PR (1995) Prostate cancer: effect of postbiopsy hemorrhage on interpretation of MR images. Radiology 195:385–390
6. Nghiem HV, Herfkens RJ, Francis IR, Sommer FG, Jeffrey RB, Li KCP, Steiner RM, Glover GH (1992) The pelvis: T2-weighted fast spin-echo MR imaging. Radiology 185:213–217
7. Kier R, Wain S, Troiano R (1993) Fast spin-echo MR images of the pelvis obtained with a phased-array coil: value in localizing and staging prostatic carcinoma. AJR 161:601–606
8. Semelka RC, Chew W, Hricak H, Tomei E, Higgins CB (1990) Fat-saturation MR imaging of the upper abdomen. AJR 155:1111–1116
9. Mirowitz SA, Heiken JP, Brown JJ (1994) Evaluation of fat saturation technique for T2-weighted endorectal coil MRI of the prostate. Magn Reson Imaging 12:743–747
10. Hardy PA, Recht MP, Piraino D, Thomasson D (1996) Optimization of a dual echo in the steady state (DESS) free-precession sequence for imaging cartilage. J Magn Reson Imaging 6:329–335
11. Ikonen S, Kärkkäinen P, Kivisaari L, Salo JO, Taari K, Vehmas T, Tervahartiala P, Rannikko S (1998) Magnetic resonance imaging of clinically localized prostatic cancer. J Urol 159:915–919
12. Quinn SF, Franzini DA, Demlow TA, Rosencrantz DR, Kim J, Hanna RM, Szumowski J (1994) MR imaging of prostate cancer with an endorectal surface coil technique: correlation with whole-mount specimens. Radiology 190:323–327
13. Hricak H, White S, Vigneron D, Kurhanewicz J, Kosco A, Levin D, Weiss J, Narayan P, Carroll PR (1994) Carcinoma of the prostate gland: MR imaging with pelvic phased-array coils versus integrated endorectal-pelvic phased-array coils. Radiology 193:703–709
14. Schiebler ML, Schnall MD, Pollack HM, Lenkinski RE, Tomaszewski JE, Wein AJ, Whittington R, Rausching W, Kressel HY (1993) Current role of MR imaging in the staging of adenocarcinoma of the prostate. Radiology 189:339–352
15. Hawass NED (1997) Comparing the sensitivities and specificities of two diagnostic procedures performed on the same group of patients. Br J Radiol 70:360–366
16. Altman DG (1991) Practical statistics to medical research. Chapman and Hall, London
17. Jager GJ, Ruijter ET, Van de Kaa CA, Rosette JJ de la, Oosterhof GO, Thornbury JR, Barentsz JO (1996) Local staging of prostate cancer with endorectal MR imaging: correlation with histopathology. AJR 166:845–852
18. Perrotti M, Kaufman RP, Jennings TA, Thaler HT, Soloway SM, Rifkin MD, Fisher HAG (1996) Endo-rectal coil magnetic resonance imaging in clinically localized prostate cancer: Is it accurate? J Urol 156:106–109
19. Yu KK, Hricak H, Alagappan R, Chernoff DM, Bacchetti P, Zaloudek CJ (1997) Detection of extracapsular extension of prostatic carcinoma with endorectal and phased-array coil MR imaging: multivariate feature analysis. Radiology 202:697–702